Studies on Synthesis and Function of Selenocysteine-containing Peptides

Tadao Oikawa

1992

Studies on Synthesis and Function of Selenocysteine-containing Peptides

Tadao Oikawa

1992

CONTENTS

	Page
ABBREVIATIONS	2
INTRODUCTION	3
CHAPTER I Metalloselenonein, the selenium analogue of metallothionein: Synthesis and characterization of its complex with copper ions	
Section 1 Synthesis of metalloselenonein	7
Section 2 EXAFS study on Cu-bound metalloselenonein	23
CHAPTER II Synthesis and characterization of a selenium analogue of glutathione, glutaselenone	
Section 1 Synthesis of glutaselenone	38
Section 2 Glutathione peroxidase activity of glutaselenone	54
ACKNOWLEDGEMENTS	64
REFERENCES	66

ABBREVIATIONS

Boc: *t*-Butyloxycarbonyl

CD: Circular dichroism

DIEA: N, N-Diisopropylethylamine

DMF: Dimethylformamide

EDTA: Ethylenediamine tetraacetic acid

EXAFS: X-ray absorption fine structure

HPLC: High performance liquid chromatography

MT: Metallothionein

NADP: Nicotinamide adenine dinucleotide phosphate

Secys: Selenocysteine

SeMT: Metalloselenonein

TFA: Trifluoroacetic acid

Tris: Tris (hydroxymethyl) amino methane

XANES: X-ray absorption near edge structure

INTRODUCTION

Selenium is located between sulfur and tellurium in the Periodic Table and has been classified both as a metal and a nonmetal. It resembles sulfur in physiological and chemical properties (Table 1, (1)).

Selenium has been known as one of the most toxic elements, causing "alkali disease" or "blind staggers" (2). In 1943, Nelson and his co-workers reported that selenium ingested as a seleniferous wheat and corn caused a high incidence of liver cancer in rats (3). However, selenium is now generally recognized as an essential micronutrient for mammals, birds, and several bacteria. The first evidence for selenium to be an essential micronutrient was described by Schwartz and Forts when a selenium-containing factor, which prevented necrotic liver degeneration in rats fed a selenium deficient diet, was isolated (4). Since then, a variety of disease syndromes that could be prevented by the administration of a small amount of selenium (5-6). In 1970's, Rotruck showed that selenium supply correlated with the enzyme activity of the glutathione peroxidase in rat erythrocytes, and identified selenium as a component of the active site of this enzyme (7). Several selenium-dependent enzymes have been found from prokaryotic organisms (Table 2). Many of these enzymes have been shown to contain selenium as a selenocysteine residue. Recently, the genes of formate dehydrogenase of *Escherichia coli* (17) and glutathione

Table 1. Comparison of Properties of S and Se.

Properties	S	Se
Atomic weight	32.06	78.96
Natural isotopes (%)	32 (95.1)	74 (0.87); 76 (9.02)
	33 (0.74)	77 (7.58); 78 (23.52)
	34 (4.18)	80 (49.82); 82 (9.19)
Covalent radius (Å)	1.06	1.16
Ionic radius (Å) (X^-)	1.84	1.98
Energy bond (KJ/mol)		
X-X bond	212.9	184.5
C-X bond	272	243
pKa ($RXH \rightleftharpoons RX^- + H^+$)		
R = -H	6.94	3.88
R = $-CH_2CH(NH_2)COOH$	8.4	5.25
Redox potential		
($H_2X(aq.) \rightleftharpoons X^0 + 2H^+ + 2e^-$)	0.23	0.30
Solubility (pH 7.0, 25°C)		
($HXCH_2CH(NH_2)COOH$) (mM)	0.38	2.35

peroxidase of human, bovine and mouse (18) were cloned. It was shown that the opal nonsense codon, TGA, encodes selenocysteine.

Then, what are the advantages of using selenocysteine residue in these enzymes? The characteristic properties of selenocysteine are as follows (19). (a) Organo selenium compounds are generally more reactive than the corresponding sulfur compounds. (b) In contrast to thiols (RSH), selenols (RSeH) are mostly ionized at neutral pH, therefore selenols in enzymes are probably be acidic. (c) Selenols are strong nucleophiles and serve as good leaving groups. (d) The lower redox potential of selenol as compared with the corresponding thiol (e.g. selenocysteine vs. cysteine) may explain the occurrence of selenols in redox catalysts such as formate dehydrogenase in strictly anaerobic bacteria.

Recently, tetraiodothyrosine 5'-deiodinase, a new selenoenzyme, was found to catalyze the conversion of thyroxine to the active thyroid hormone (20). A new mammalian selenoprotein P, which contains at least 8 selenocysteine residues per subunit, is also of physiological importance, although its biochemical function remains to be clarified (21). Therefore, the synthetic selenoproteins and peptides are expected to show interesting physiological functions, but their facile synthesis is not available.

Table 2. Selenium-containing proteins.

Enzyme	Selenium	origin	Reference
Glutathione peroxidase	SeCys	Bovine erythrocyte	8
Glycine reductase	SeCys	*Clostridium sticklandii*	9
Foramte dehydrogenase	SeCys	*Methanococcus vanielii*	10
	SeCys	*C. thermoaceticum*	11
	unknown	*E. coli*	12
Xanthine dehydrogenase	unknown	*C. acidiurici*	13
	unknown	*C. cylindrosporum*	14
Nicotinate hydroxylase	labile	*C. barkeri*	15
Thiolase	SeMet	*C. kluyveri*	12
Hydrogenase	SeCys	*M. vanielii*	16

In this thesis, I describe the synthesis and characterization of a selenium analogue of a *Neurospora crassa* copper metallothionein and glutathione. I have established a method to introduce selenium into an usual non-selenoprotein and peptides by solid or liquid-phase peptide synthesis.

CHAPTER I

Metalloselenonein, the selenium analogue of metallothionein: Synthesis and characterization of its complex with copper ions

Section 1. Synthesis of metalloselenonein

A selenocysteine residue occurs as an integral moiety in the active center of the selenium-containing enzymes such as glycine reductase, formate dehydrogenase, and glutathione peroxidase (22). The catalytic role of the selenocysteine residue is attributed to the high reactivity of the selenol group of the selenocysteine residue: selenols have much lower redox potentials than the sulfur counterparts (19). Thus, attention has been paid to synthesis of selenocysteine-containing polypeptides and proteins which may have unique properties that the sulfur counterparts do not have (23).

Metallothioneins are cysteine-rich proteins with low molecular weights, that bind various kinds of metal ions (24). The biological functions of metallothioneins have been proposed to be involved in provision of physiological metals for metalloenzymes, and storage and detoxification of heavy metal. These functions depend on their high affinity to metal ions and the reactivity of cysteine residues in a metal-thiolate cluster. I here describe synthesis of metalloselenonein, in which all the

cysteine residues in the *Neurospora crassa* copper metallothionein are replaced by selenocysteines, and its interaction with copper ions.

EXPERIMENTAL PROCEDURES

Materials

L-β-Chloroalanine was synthesized from L-serine (25); disodium diselenide was prepared by the method of Klayman and Griffin (26); L-selenocysteine was prepared from disodium diselenide and L-β-chloroalanine (27); *Se*-(*p*-methylbenzyl)-L-selenocysteine was obtained from L-selenocysteine and α-bromo-*p*-xylene by a modification of the procedure of Erickson and Merrifield (28); *Se*-(*p*-methylbenzyl)-*N*-*t*-Boc-L-selenocysteine was prepared from *Se*-(*p*-methylbenzyl)-L-selenocysteine and *S*-*t*-Boc-4,6-dimethyl-2-thiopyrimidine by a modification of the procedure of Nagasawa et al. (29). Other reagents, the best grade commercially available, were used without further purification.

Synthesis of Metalloselenonein

Metalloselenonein was synthesized in an Applied Biosystems 430A peptide synthesizer programmed as shown in Table 3. The synthesis was started on 1 g of $N\alpha$-*t*-Boc-Lys-(Cl-Z)-OCH_2-Pam resin (0.5 mmol/g of resin) (30). The *t*-butyloxycarbonyl (Boc) group was used for the $N\alpha$-terminus, and the side-chain

Table 3. Solid-phase synthesis protocol.

Step	Reagents and operation	Mixing time (min)
1. Deprotection	60% CF_3COOH in DMF	1
2. Wash	CH_2Cl_2 (three times)	1
3. Neutralization	10% DIEA in DMF (twice)	1
4. Wash	DMF (six times)	1
5. Coupling	Symmetric anhydride method in DMF	20
6. Wash	DMF (twice)	1
	CH_2Cl_2 (four times)	1
7. Ninhydrin test		

DMF, dimethylformamide; DIEA, *N*, *N*-diisopropylethylamine

protections were as follows: Asp(OBzl), SeCys(MeBzl), and Ser(OBzl) (Bzl, benzyl; MeBzl, methyl benzyl). The coupling reactions were carried out with 2.0 mmol of protected amino acid. The yield in the coupling reaction was determined with ninhydrin (31).

Deprotection and purification of metalloselenonein

The peptidyl resin produced (about 1.0 g) was treated with anhydrous hydrogen fluoride containing 15% anisole and 2.5% ethyl methyl sulfide at 0°C for 1 h. After evaporation of hydrogen fluoride, the residue was washed with diethyl ether and extracted with 2 M acetic acid, and the extract was lyophilized.

The crude peptide was purified by reversed phase high performance liquid chromatography (HPLC). Special care was taken to avoid air oxidation during the purification procedure. All buffers were kept under constant stream of nitrogen. Preparative separations were done with an Ultron C18 column (Shinwakako, Kyoto, Japan; 25 X 1 cm) at a flow rate of 2.4 ml/min, while analytical separations were carried out on an Ultron N-C18 column (15 X 0.46 cm) at a flow rate of 0.8 ml/min. Both columns were programmed with a 30 min linear gradient from 5 to 50% acetonitrile in water. Trifluoroacetic acid was added at a concentration of 0.1% (v/v) to water and acetonitrile. Peptides were detected at 210 nm.

Amino Acid Analysis

Amino acid analysis was performed with a Beckman 7300 amino acid analyzer. Peptides were hydrolyzed in 6 M HCl (Pierce Chemical) at 108°C in a sealed vessel under reduced pressure for 9 h with a Waters PICO-TAG automatic acid hydrolysis system. Selenocysteine was determined after conversion into *Se*-carboxymethyl selenocysteine with iodoacetic acid. Amount of amino acid residues were calculated on the basis of molecular weight of 2,548 for metalloselenonein.

Preparation of apometalloselenonein and Cu-bound metallselenonein (Cu-SeMT)

All procedures were performed in a nitrogen glove box in which oxygen concentration was kept below 10 ppm. All solutions were evacuated prior to use. Metalloselenonein (390 nmole) was incubated in 20 mM Tris-HCl buffer (pH 8.6) containing 5.85 μmole of $CuCl_2$ and 1.2 mmole of β-mercaptoethanol at 30°C for 30 min. The solution was applied to an Asahipak GS-220 HPLC column (500 X 7.6 mm; Asahi-Kasei, Tokyo, Japan) equilibrated with 20 mM Tris-HCl buffer (pH 8.6).

Analytical methods

Absorption spectra were recorded using a Shimadzu MPS-2000 spectrophotometer in a sealed cuvette under reduced pressure. Circular dichroism spectra were recorded in a Jasco J-600 spectropolalimeter using 1-mm cuvette at room temperature (about

20°C). Fluorescence spectra were measured using a Hitachi MPF-4 fluorescence spectrophotometer at 25°C. The copper content was determined by the method of standard additions with a Shimadzu AA-670G atomic absorption spectrophotometer equipped with a graphite furnace atomizer. Absorption was monitored at 324.8 nm with deuterium arc background correction. I took an average of three independent determinations. All solutions used for copper analysis were passed through a Chelex (Bio-Rad) column (1 X 10 cm) to remove free copper ions, and stored in polyethylene bottles.

RESULTS

Synthetic strategy

I synthesized metalloselenonein by solid-phase method (32) with an automated peptide synthesizer. Its sequence is H-GLY-ASP-SECYS-GLY-SECYS-SER-GLY-ALA-SER-SER-SECYS-ASN-SECYS-GLY-SER-GLY-SECYS-SER-SECYS-SER-ASN-SECYS-GLY-SER-LYS-OH, where SECYS means selenocysteine. The *N*α-amino terminus and the side chains of amino acids were protected with acid-labile groups: *N*α-amino terminus, *t*-butyloxycarbonyl group; aspartic acid and serine, benzyl group. However, no masking group for the selenol of selenocysteine has been developed. I used a *p*-methylbenzyl group to protect the selenol of selenocysteine. Several new techniques have been developed to reduce side reactions during the peptide

synthesis and were used in the present synthesis. For example, Pam resin, which has acid-stable linkage to the resin support, was used to reduce loss of premature peptides during acidolytic deprotection cycles (33, 34). I used symmetrical anhydride coupling in dimethylfomamide for 20 min to obtain satisfactory coupling yields of more than 99% for all coupling steps except for the step of Ala^{8}-Ser^{9} synthesis: only 96.7% coupling yields were achieved.

Purification of metalloselenonein

Metalloselenonein synthesized as described above was purified by preparative HPLC after reduction with $NaBH_4$. The final preparation of metalloselenonein was eluted as a single symmetrical peak upon analytical HPLC (Fig. 1), and was found to be homogeneous by amino acid analysis of the acid hydrolysates (Table 4). The overall recovery in the preparative HPLC was about 2%. The low yield is probably attributable to the irreversible adsorption of metalloselenonein to the HPLC column. Selenocysteine is oxidized to give selenocysteic acid by performic acid oxidation in the same manner as cysteine. However, selenocysteic acid is decomposed during acid hydrolysis of proteins (35). Therefore, I analyzed selenocysteine in the form of *Se*-carboxymethyl selenocysteine after alkylation with iodoacetic acid.

Selenium compounds are generally highly susceptible to oxidative degradation. However, I have found that the selenol of

metalloselenonein is oxidized much more slowly than that of selenocysteine. When metalloselenonein (0.4 mM was incubated in 0.1 M Tris-HCl buffer (pH 8.0) at 37°C for 2 h, all of the initial selenocysteine residues remained intact, whereas 52% of free selenocysteine was oxidized to selenocystine under the same conditions.

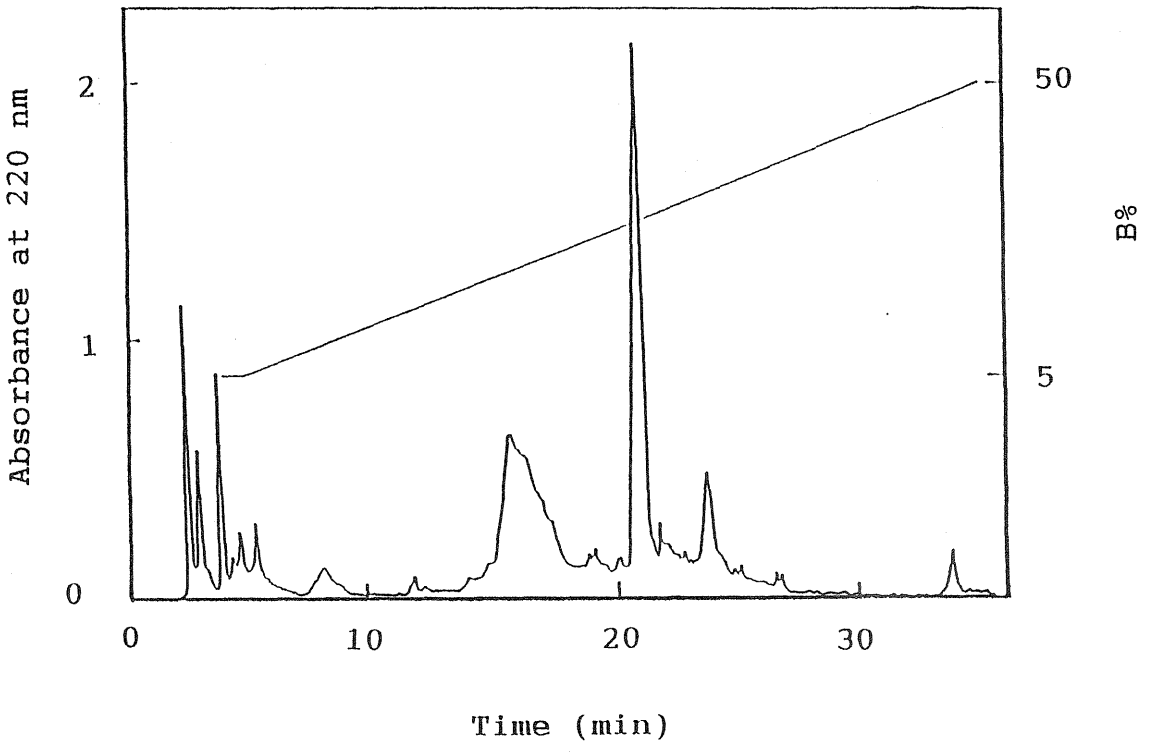

Fig. 1. Reversed phase HPLC profile of metalloselenonein. The crude peptide was applied to a column equilibrated with 0.1% trifluoroacetic acid in 5% acetonitrile. The column was washed with the same buffer at a flow rate of 0.8 ml per min followed by elution with a linear gradient between 0.1% trifluoroacetic acid in water and 50% acetonitrile containing 0.1% trifluoroacetic acid (B%).

Table 4. Amino acid analysis of metalloselenonein

Amino Acid	Number of residues	
	Calculated	Found
Ala	1	1.0
Asx	3	2.4
Gly	6	6.0
Lys	1	0.7
SeCys[1)]	7	7.1
Ser	7	6.6

1) Determined as *Se*-carboxymethyl selenocysteine after alkylation with iodoacetic acid.

Spectroscopic properties of Cu-bound metalloselenonein

The metalloselenonein complex with Cu(I) was isolated by HPLC with an Asahipak GS-220 gel filtration column. The first major fraction (*Mr*, about 2,700) contained 3 gram atoms of copper per mol. The absorption spectrum of the copper complex was characterized by a broad absorption band between 230 and 400 nm with a shoulder around 260 nm (Fig. 2). However, metalloselenonein itself showed no absorption above 260 nm.

Therefore, the broad absorption band around 260 nm observed for the copper complex is most probably attributed to a copper-selenolate complex. The circular dichroism of the copper-metalloselenonein complex revealed a negative band at 220 nm and a positive band at 245 nm (Fig. 2). Metalloselenonein itself showed only a negative band at 220 nm, which is attributable to an amide transition. Therefore, the positive band at 245 nm shows asymmetry in the copper-selenolate coordination. The copper-metalloselenonein complex showed an emission spectrum with a maximum at 395 nm when it was excited at 245 nm (Fig. 3). Addition of 1 M HCl to the solution containing the complex led to complete disappearance of not only the absorption band around 260 nm but also the fluorescence band at 395 nm. This indicates displacement of copper with protons in the complex upon addition of HCl. Furthermore, both electron-spectral bands were lost when the complex was oxidized in air.

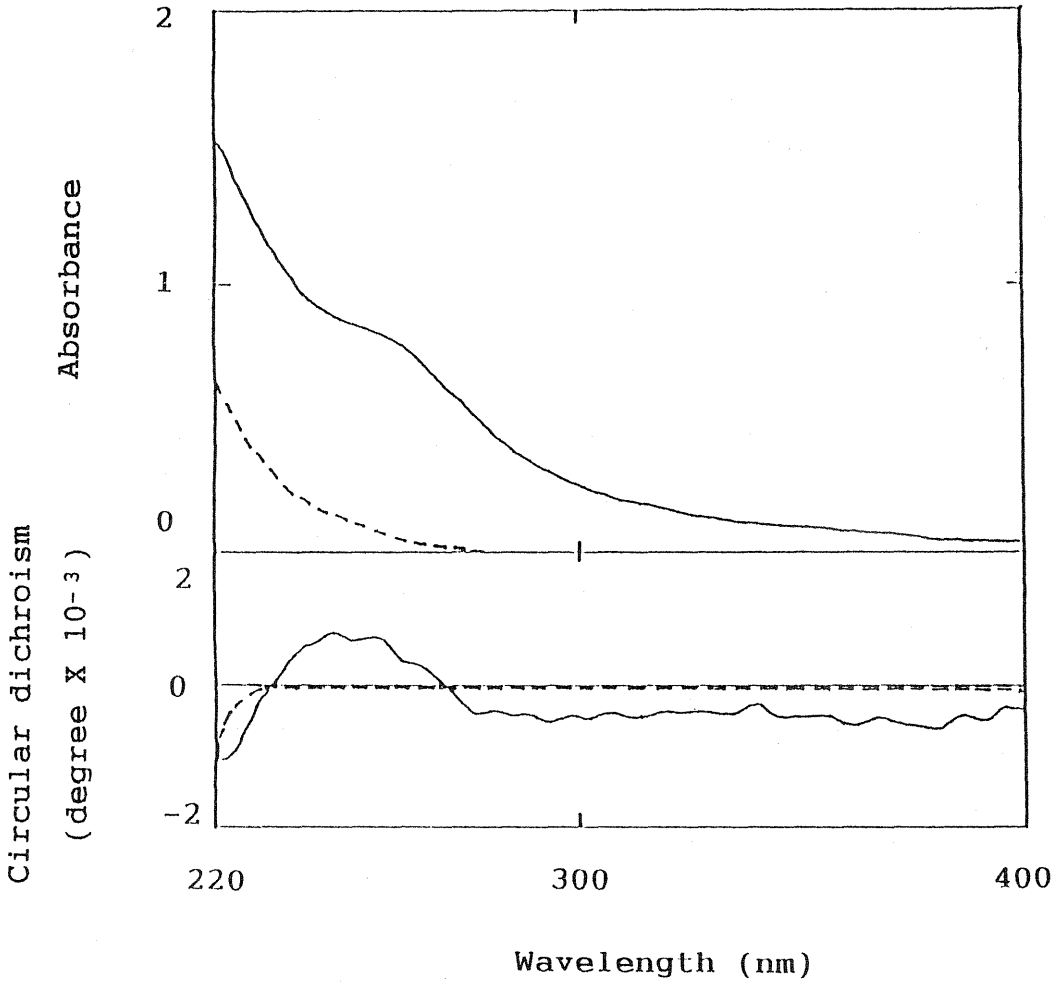

Fig. 2. Absorption spectra and circular dichroism of metalloselenonein. The solid line shows the spectrum of the copper complex of metalloselenonein in 20 mM Tris-HCl buffer (pH 8.6), and the dotted line shows the spectrum of metalloselenonein in 50 mM HCl.

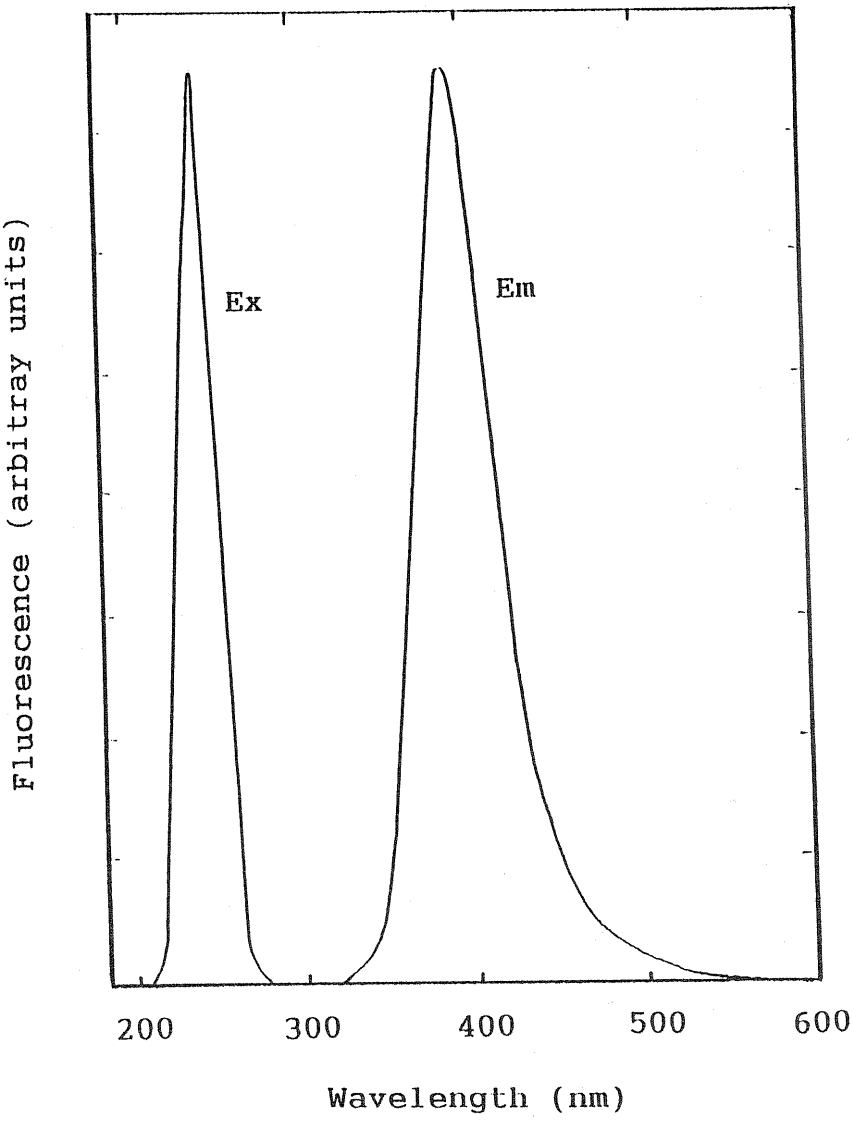

Fig. 3. Fluorescence spectrum of copper-metalloselenonein complex.

DISCUSSION

The selenium analogues of various sulfur-containing peptides and proteins have been prepared previously. The acid-labile sulfur in several iron-sulfur proteins was replaced by selenium: Fe_2S_2 putidaredoxine (36) and parsley ferredoxin (37); Fe_4S_4 ferredoxin from *Clostridium pasteurianum* (38). A derivative of β-galactosidase whose methionine residues were extensively replaced by selenomethionine residues was obtained from a selenium-resistant mutant of *E. coli* grown on sodium selenate. Selenium analogues of glutathione (39), oxytocin (40), and somatostatin (41) were synthesized by the manual liquid-phase method (42), which is much less efficient than the automatic solid-phase method based on symmetric anhydride coupling chemistry. I have achieved the synthesis of a metalloselenonein that contains selenocysteine residues for all cysteine residues in copper metallothionein of *N. crassa*, with an automatic peptide synthesizer according to the standard protocol.

The Cu-metalloselenonein in complex showed a broad absorption band between 230 and 400 nm with a shoulder around 260 nm. This is probably attributable to Se*-Cu(I) transition in the copper-selenolate complex. The circular dichroism spectrum of the Cu-metalloselenonein complex showed a positive CD band around 245 nm. This indicates asymmetry in the copper-selenolate complex because the CD band is absent in free metalloselenonein. The fluorescence spectrum of the copper-metalloselenonein complex

is also attributable to transitions of a charge-transfer type of the Cu(I)-selenolate complex. Metalloselenonein binds 3 copper ions per mol in contrast to the native and reconstituted metallothionein of *N. crassa* which binds 6 copper ions per mol (43, 44). In the copper complex of metallothionein, copper atoms are contained in a compact polynuclear cluster with the thiolate of the cysteine residues (45). The difference in ionic radius between sulfur and selenium (46) most likely accounts for the observed difference in the coordination mode between the two copper-complexes.

SUMMARY

I synthesized a selenocysteine-containing peptide, metalloselenonein, which contains selenocysteine residues substituted for all cysteine residues in *Neurospora crassa* copper metallothionein, using an automated peptide synthesizer. Metalloselenonein binds 3 gram atoms of Cu(I) per mol. This adduct showed a broad absorption band between 230 and 400 nm and a fluorescence band at 395 nm, which can be attributed to copper-selenolate coordination. The circular dichroism spectrum of the Cu-metalloselenonein complex showed a positive CD band around 245 nm attributable to asymmetry in metal coordination.

Section 2. EXAFS study on Cu-bound metalloselenonein

The phenomenon of Extended X-ray Absorption Fine Structure (EXAFS) was first treated theoretically by Kroning in the 1930s. Recent developments, initiated by Sayers, Stern, and Lytle in the early 1970s, have led to the recognition of the structural content of this technique. At the same time, the availability of synchrotron radiation has greatly improved both the acquisition and the quality of the EXAFS data over those obtainable from conventional X-ray sources. Such developments have established EXAFS as a powerful tool for structure studies.

EXAFS has been successfully applied to a wide range of significant scientific and technological systems in many diverse fields such as inorganic chemistry, biochemistry, catalysis, material sciences, etc. It is extremely useful for systems where single-crystal diffraction techniques are not readily applicable (e.g., gas, liquid, solution, amorphous and polycrystalline solids, surfaces, polymer etc.).

EXAFS refers to the oscillatory variation of the X-ray absorption as a function of photon energy beyond an absorption edge (Fig. 4). The absorption, normally expressed in terms of absorption coefficient (μ), can be determined from a measurement of the attenuation of X-rays upon their passage through a material (47). When the X-ray photon energy (E) is tuned to the X-ray absorber, the light scattering occurs (Fig. 5). The outgoing photoelectron waves from the X-ray absorbing atom are

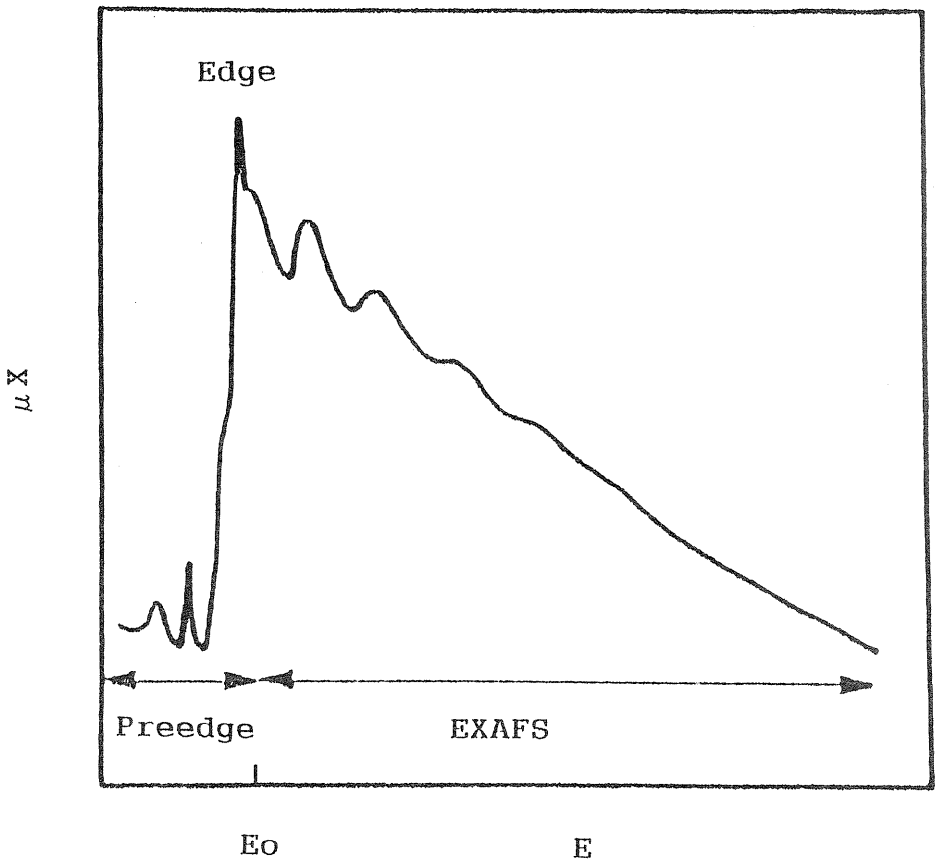

Fig. 4. Schematic representation of the transmission experiment and the resulting X-ray absorption spectrum μx *vs* E for an absorption edge of the absorbing atom.

backscattered by the neighboring atoms to form the incoming photoelectron waves to the X-ray absorbing atom. The final state is the total of the outgoing photoelectron waves from the X-ray absorbing atom and all the incoming photoelectron waves from each neighboring atom. This interference between the outgoing and incoming photoelectron waves gives rise to the sinusoidal curve above the absorption edge (Fig. 4).

The EXAFS provides the information about the radial distributions of the atoms around the X-ray absorber: the number and kind of the neighboring atoms, and their distances away from the X-ray absorber. Therefore, the other substances or elements, which either do not contain the X-ray absorber or are not directly bound to the X-ray absorber, do not affect the EXAFS. Moreover, the EXAFS analysis can be applied to all the samples in the solid (crystalline or amorphous), liquid, or gas with the same accuracy (0.01-0.03 Å). Since the Se K-edge and L-edge are observed in the EXAFS region (Table 5), the structure of Cu-bound metalloselenonein can be determined by Se-EXAFS. Therefore, I have studied Cu and Se EXAFS of Cu-bound metalloselenonein.

Table 5. The absorption edges of the various physiologically active elements.

Element	Absorption edges (kX/1.002) K-edge	L-edge
K	3.43645	42.17
Ca	3.07016	35.49
Mn	1.896	19.40
Fe	1.743	17.53
Co	1.608	15.93
Ni	1.488	14.579
Cu	1.380	13.288
Zn	1.283	12.130
Se	0.979	8.645
Mo	0.61977	4.912

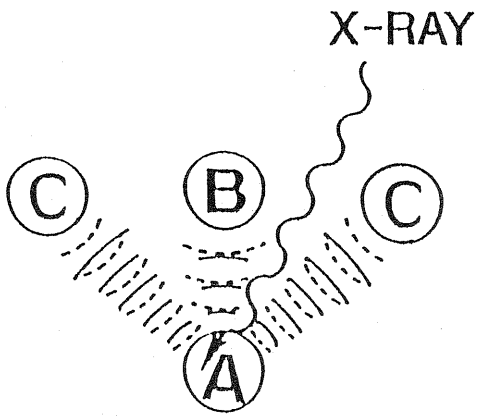

A: Absorbing Atom

B, C: Neighboring Atom

$$\chi(k)=\sum_j \frac{N_j}{kR_j^2}\left|f_j(\pi)\right|\sin[2kR_j+2\delta_1'+\psi_j(k)]e^{-\gamma R_j}e^{-2\sigma_j^2k^2}$$

Fig. 5. The light scattering caused by the X-ray absorption.

EXPERIMENTAL PROCEDURES

Sample Preparations

Crystalline L-selenocystine was mixed with polyethylene powder, and the pellet of the mixture was made under high pressure. The following aqueous solutions were also prepared to be analyzed: 10 mM L-selenocystine in 0.2 M 2-(N-cyclohexylamino)-ethanesulfonic acid (CHES) buffer (pH 9.5); 40 mM L-selenocystine in 0.2 M CHES buffer (pH 9.5) (selenol group of selenocysteine is dissociated under the conditions (pKa of SeH is 5.0); 40 mM L-selenocysteine in 0.5 M HCl (selenol is not dissociated under the conditions).

Cu-bound metalloselenonein: All procedures were performed in a nitrogen glove box in which oxygen concentration was kept below 10 ppm. All solutions were evacuated prior to use. Metalloselenonein (390 nmole) was incubated in 20 mM Tris-HCl buffer (pH 8.6) containing 5.85 μmole of $CuCl_2$ and 1.2 mmole of β-mercaptoethanol at 30°C for 30 min. The solution was applied to an Asahipak GS-220 HPLC column (500 X 7.6 mm; Asahi-Kasei, Tokyo, Japan) equilibrated with 20 mM Tris-HCl buffer (pH 8.6).

Data collections

The X-ray absorption spectra of selenocystine were recorded over the energy range corresponding to the selenium K-edge. Data were collected at room temperature at an energy of 2.5 GeV with an average current of 193 mA. The X-ray absorption data were

converted to EXAFS modulation spectra with a cubic spline fit background subtraction.

The X-ray absorption spectra of Cu-SeMT in the EXAFS and the X-ray absorption near edge structure (XANES) regions were measured by fluorescence mode with a Lytle detector at BL7C.

RESULTS AND DISCUSSION

EXAFS study on selenocystine

Figure 6 shows the X-ray absorption spectrum in the region of the Se K-edge for aqueous solution of L-selenocystine. Essentially identical spectrum was obtained for L-selenocystine solidified with polyethylene. The bond lengths were determined as follows: C-Se, 1.88 Å; and Se-Se, 2.32 Å. When L-selenocystine was dissolved in 0.1 M HCl and analyzed, the same EXAFS was observed. Therefore, these bond lengths were not influenced by dissociation of COOH and NH_2. Figure 7 illustrates the X-ray absorption spectrum for aqueous acidic solution of selenocysteine whose selenol group is not dissociated, while Figure 8 shows the spectrum for the alkaline selenocysteine solution in which selenol of selenocysteine is dissociated. The C-Se bond length determined were 1.96 Å for both the systems.

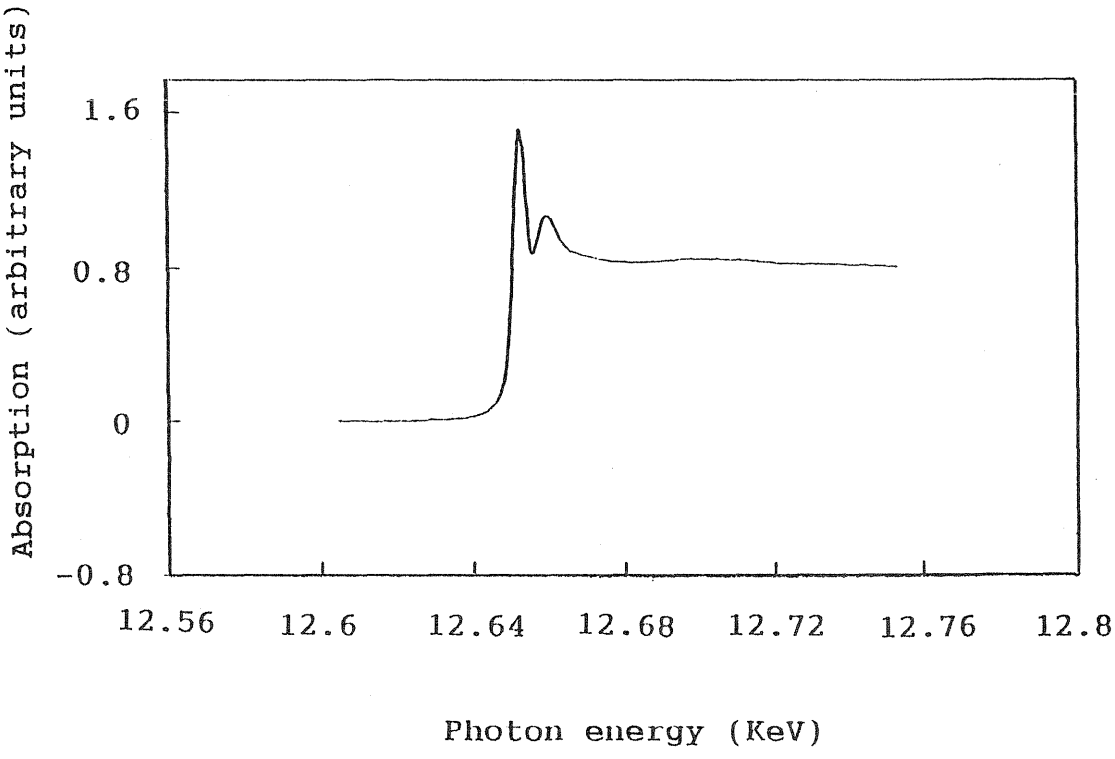

Fig. 6. Se K-edge absorption spectrum of L-selenocystine.

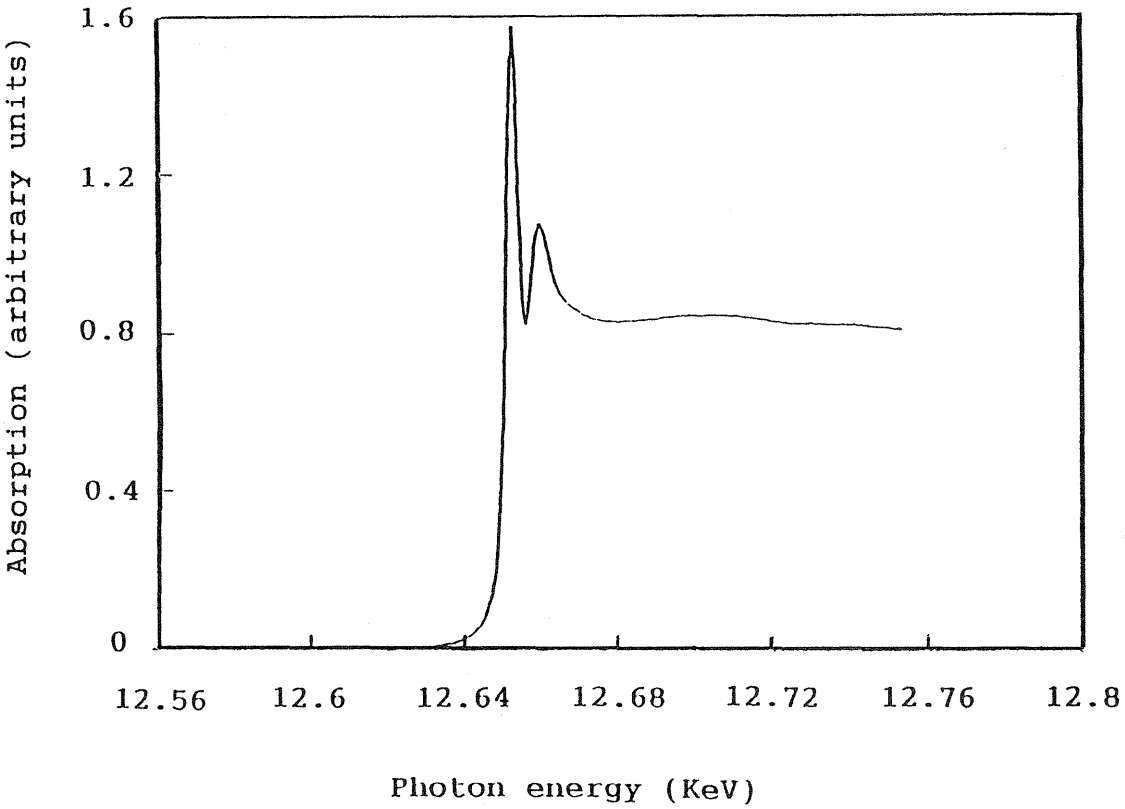

Fig. 7. Se K-edge absorption spectrum of L-selenocysteine under acidic conditions.

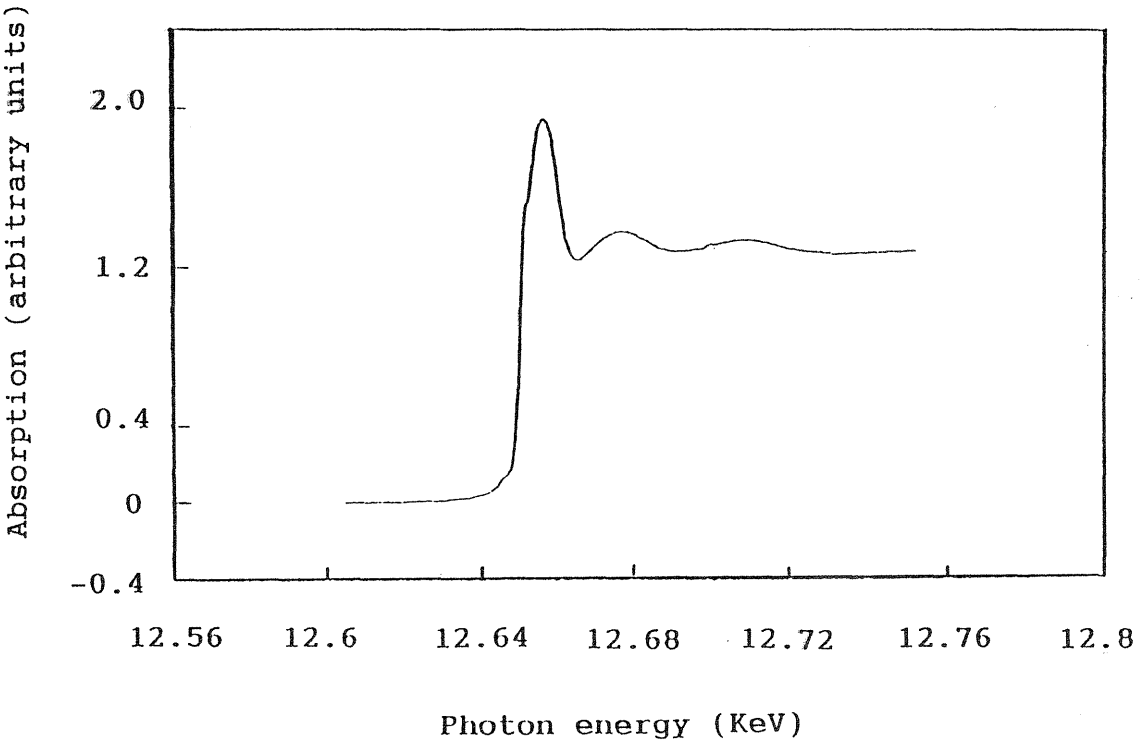

Fig. 8. Se K-edge absorption spectrum of L-selenocysteine under alkaline conditions.

EXAFS study on Cu-bound metalloselenonein

Figure 9 shows the Cu-EXAFS of Cu-SeMT. In order to determine the Cu-Se coordination mode, the EXAFS data were Fourier-transferred, and then fitted to the various models with two, three, or four Cu-Se coordinations. The four-coordinate model alone was consistent with the results of EXAFS parameters of Cu-SeMT. The Cu-EXAFS revealed that three different kinds of Cu-Se bonds occur in Cu-SeMT ($Cu\text{-}Se_{I}$, 2.31; $Cu\text{-}Se_{II}$, 2.36; $Cu\text{-}Se_{III}$, 2.58 Å), and the ratio of occurrence was 3, 1, and 3, respectively. The same results were obtained by the Se-EXAFS (Table 6). Figure 10 shows the proposed structure of Cu-SeMT. Each copper atom was coordinated to four selenium atoms at a distance of 2.31, 2.36, or 2.58 Å, and the Cu-Cu distance was 3.14 Å.

The EXAFS studies of various copper metallothioneins have been reported. Freedman and his co-workers reported EXAFS of copper metallothionein from canine liver, and concluded that the copper was coordinated to four sulfur atoms, all of which located at a distance of 2.27 Å (48). Abrahams and his co-workers recently reported the EXAFS of zinc metallothionein and mixed copper-zinc metallothionein from rabit and pig livers, respectively (49). The copper atoms were found to be coordinated to three sulfur atoms at a distance of 2.25 Å in the mixed Cu-Zn metallothionein. Smith and his co-workers examined Cu-EXAFS of *Neurospora crassa* copper metallothionein, which contains 6 copper atoms bound to the 25-mer polypeptide with 7 cysteine residues.

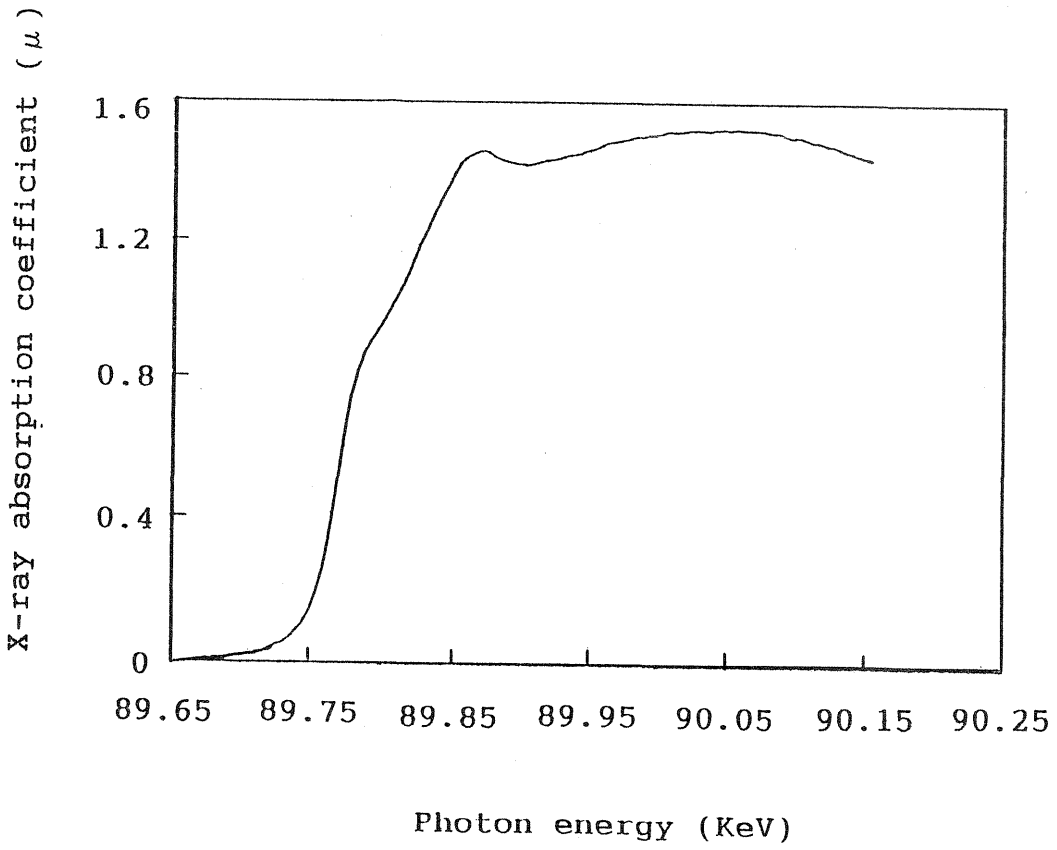

Fig. 9. XANES spectum of Cu-SeMT.

Table 6. Bond length of Cu-SeMT (Å).

	Cu-EXAFS	Se-EXAFS
$Cu-Se_{I}$	2.31	2.29
$Cu-Se_{II}$	2.36	2.29
$Cu-Se_{III}$	2.58	2.63
C-Se		1.99
Cu-Cu	3.14	
Se-Se		3.09

Their model showed the copper ions were coordinated to three or four sulfur atoms at a distance of 2.20 Å (45). The inconsistency of our model with that of Smith et al probably arose from the difference in ionic radius between sulfur and selenium.

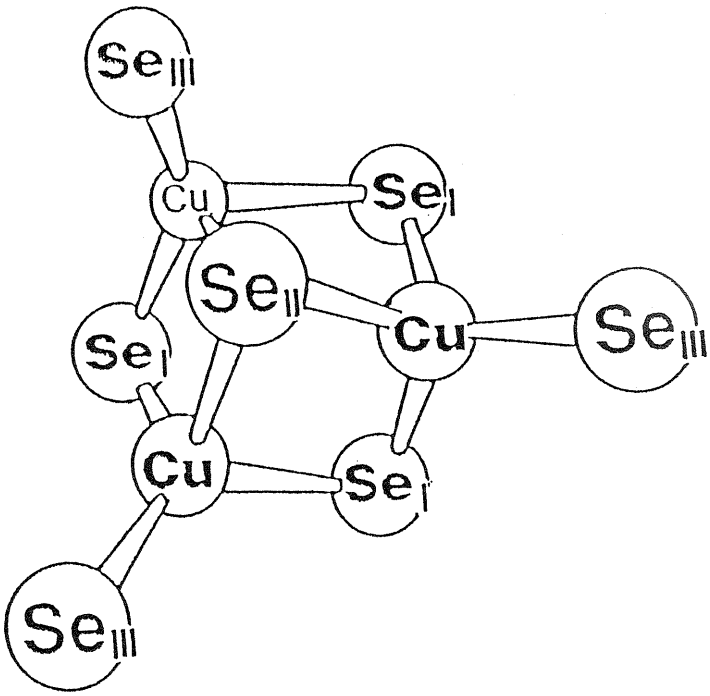

Fig. 10. Proposed Structure of Cu-SeMT.

SUMMARY

The Cu-bound metalloselenonein was analyzed by Cu- and Se-EXAFS. The results revealed that three different Cu-Se bonds occur in Cu-SeMT ($Cu\text{-}Se_{I}$, 2.31; $Cu\text{-}Se_{II}$, 2.36; $Cu\text{-}Se_{III}$, 2.58 Å), and the ratio of occurrence was 3, 1, and 3, respectively: each copper atom was coordinated to four selenium atoms at a distance of 2.31, 2.36, or 2.58 Å, and the distance between two copper atoms were 3.14 Å.

CHAPTER II

Synthesis and characterization of a selenium analogue of glutathione, glutaselenone

Section 1. Synthesis of glutaselenone

Selenocysteine residue differs from its analogue, cysteine, in its redox potential and in various other chemical properties (8, 19, 50, 51), and occurs as an integral moiety in the active center of selenium-containing enzymes, such as mammalian glutathione peroxidase (52) and bacterial glycine reductase (9). Selenocysteine-containing glutathione analogues are expected to show interesting physiological functions, but their facile synthesis has not been previously described.

Glutathione is the most predominant intracellular thiol, and has many important biochemical functions in protein and DNA syntheses, amino acid transport, and protection of cells from oxidative damage (53, 54). The functions of glutathione are based on the high reactivity of the cysteine residue.

I here describe the synthesis of each four selenium analogues of glutathione, LL, LD, DL, and DD-glutaselenone (i.e. γ-L-glutamyl-L-selenocysteinylglycine) separately, and their characterization spectroscopically.

EXPERIMENTAL PROCEDURES

Materials

β-Chloro-L-alanine and β-chloro-D-alanine were synthesized from L-serine and D-serine, respectively (25); disodium diselenide was from elemental selenium (26); L-selenocystine and D-selenocystine was from disodium diselenide and β-chloro-L-alanine and β-chloro-D-alanine, respectively (27), and *Se-p*-methoxybenzyl-L-selenocysteine and *Se-p*-methoxybenzyl-D-selenocysteine was from L-selenocystine and D-selenocystine, sodium borohydride and *p*-methoxybenzyl chloride, respectively (28). The oxidized form of glutathione was purchased from Kojin Chemical Co. (Tokyo, Japan). Other reagents were of analytical grade.

Synthesis of N-p-methoxybenzyloxycarbonyl-Se-p-methoxybenzyl-selenocysteine (Z(OCH_3)-SeCys(MBzl)-OH)

Se-p-Methoxybenzyl-L-selenocysteine (4.0 g) was dissolved in water (50 ml) containing triethylamine (4.2 ml) at 0°C. Then, *p*-methoxybenzyl azideformate (4.3 g) dissolved in dioxane (50 ml) was added to the solution. After 16 hr, the solvent was removed under reduced pressure, and the residue was dissolved in saturated citric acid solution (200 ml). The precipitate was collected by filtration, and washed with 5% citric acid and water. The product was dissolved in minimum volume of ethyl acetate, then crystallized by the addition of *n*-hexane. (yield:

80%). The D-isomer of Z(OCH_3)-Secys(MBzl)-OH was synthesized with *Se-p*-methoxybenzyl-D-selenocysteine in the same manner. The yield was 78%.

Synthesis of benzyl N-p-methoxybenzyloxycarbonyl-Se-p-methoxybenzyl-selenocysteinyl-glycinate (Z(OCH_3)-SeCys(MBzl)-Gly(OBzl)-OH)

A solution of glycine benzyl ester *p*-toluenesulfonate salt (6.26 g) in dimethylformamide (40 ml) containing triethylamine (1.34 ml) was added to a mixture of Z(OCH_3)-L-SeCys(MBzl)-OH (4.0 g), *N*, *N*'-dicyclohexylcarbodiimide (2.0 g), 1-hydroxybenzotriazole (1.34 g), and dimethylformamide (40 ml) at 0 °C. After 16 hr, the solvent was removed under reduced pressure, and the residue was dissolved in ethyl acetate (100 ml). After the mixture was washed successively with 5% citric acid, saturated sodium chloride solution, and 5% sodium bicarbonate, the ethyl acetate layer was dried over anhydrous magnesium sulfate, and evaporated. The product after dissolved in minimal amount of ethyl acetate was crystallized by the addition of ethyl ether (yield: 83%). The D-isomer of Z(OCH_3)-SeCys(MBzl)-Gly(OBzl)-OH was obtained with Z(OCH_3)-D-SeCys(MBzl)-OH in the same manner. The yield was 88%.

Synthesis of benzyl N-t-buiyloxycarbonyl-γ-glutamyl (α-benzyl ester)-Se-p-methoxybenzyl-selenocysteinyl-Glycinate (Protected glutaselenone)

Z(OCH_3)-L-SeCys(MBzl)-Gly(OBzl)-OH (1.8 g) was treated with trifluoroacetic acid (6 ml) containing anisole (1 ml) at 0°C for 1 hr. The oily residue obtained after evaporation was washed with *n*-hexane by decantation. The residue dried under reduced pressure was dissolved in dimethylformamide (20 ml), and reacted with α-benzyl-γ-*N*-hydroxysuccimide ester-*N*-*t*-butyloxycarbonyl-glutamic acid [prepared from *N*-*t*-butyloxycarbonyl-L-glutamic acid α-benzyl ester and 1-hydroxysuccimide (55)] (1.38 g) in the presence of triethylamine (0.42 ml). After 16 hr, the solvent was removed under reduced pressure, and the residue was dissolved in ethyl acetate (100 ml). After the mixture was washed successively with 5% citric acid, saturated sodium chloride solution, and 5% sodium bicarbonate, the ethyl acetate layer was dried with anhydrous magnesium sulfate. The solvent was evaporated, and the solid residue obtained was dissolved in minimal amount of ethyl acetate, then added *n*-hexane slowly to crystallize (yield: 60%). The other diastereoisomers of protected glutaselenone were synthesized by the same way. The yield were as follows: DL-isomer, 77%; LD-isomer, 68%; DD-isomer, 72%.

Deprotection of the protected glutaselenone with trimethylsilyl bromide

All procedures were carried out in a chamber with sufficient ventilation. The protected glutaselenone (100 mg) was treated with *m*-cresol (488 μl) and thioanisole (1.2 ml) in a glass

centrifuge tube (50 ml) closed with a $CaCl_2$ plug at 0°C for 5 min. Trifluoroacetic acid (3.75 ml) was added to the mixture slowly with stirring. After 5 min, trimethylsily bromide (0.66 ml) was added, and the mixture was reacted at 25°C for 24 hr with vigorous stirring. The reaction mixture was evaporated under reduced pressure without heating for 30 min. The oily residue obtained was washed three times with ice cooled diethyl ether (50 ml) by decantation. The residue after dried under reduced pressure was dissolved in water (2 ml), and the aqueous solution was neutralized with 5% NH_4OH to form diselenide form of glutaselenone. The solution was applied to a column of Sephadex G-10 (10 X 500 mm) equilibrated with 1 M acetic acid. Fractions containing an oxidized form of glutaselenone eluted with the same solution were combined and lyophilized to give a fluffy powder.

Analytical methods

I measured the melting points with micro melting point analyzer (Yanagimoto, Japan). I measured optical rotations with an automatic polarimeter, model DIP-360 (Japan Spectroscopic Co.) at 25°C. Elemental analysis was done with Yanako CHN corder, model MT-3 (Yanagimoto, Japan). Absorption spectra were taken with a Shimadzu MPS-2000 spectrophotometer. Fluorescence spectra were measured with a Hitachi MPF-4 fluorescence spectrophotometer at 20°C. Circular dichroism spectra were recorded in a model J-600 spectropolarimeter (Japan Spectroscopic Co.) using 1-mm cuvette at room temperature. Analytical separations were done

with a COSMOSIL 5C18-AR column (4.6 X 150 mm, Nacalai Tesque, Kyoto, Japan) at a flow rate of 1.0 ml/min. The column was programmed with a 30 min linear gradient from 0 to 50% acetonitrile in water. Trifluoroacetic acid was added at a concentration of 0.1% (v/v) to water and acetonitrile. Peptides were detected at 220 nm. The amino acid analysis was performed with a Beckman 7300 amino acid analyzer. Peptides were hydrolyzed with 4 M methanesulfonic acid (Pierece Chemical Co.) at 110°C in a sealed vessel under reduced pressure for 1 hr with a Waters PICO-TAG acid hydrolysis system (56). The methanesulfonic acid solution was neutralized with 3.5 M NaOH before application to the amino acid analyzer.

RESULTS AND DISCUSSION

I have synthesized separately each four diastereoisomers of glutaselenone by liquid phase method. Their sequences were as follows: H-γ-L-Glu-L-Sec-Gly, H-γ-L-Glu-D-Sec-Gly, H-γ-D-Glu-L-Sec-Gly, and H-γ-D-Glu-D-Sec-Gly, where Sec means selenocysteine. The *N*α-amino terminus and the side chain of amino acids were protected with acid-labile groups: *N*α-amino terminus, *t*-butyloxycarbonyl and *p*-methoxybenzyloxycarbonyl group; glutamic acid and glycine, benzyl group. I have protected the selenol group of selenocysteine with *p*-methoxybenzyl group (57). The benzyl group has been previously used to protect the selenol

group of selenocysteine in the peptide synthesis. *Se*-Benzyl group is generally removed by the reduction with sodium in liquid ammonia, but side reactions occur (58, 59). In contrast, the *p*-methoxybenzyl group, which I used for protection of the selenol group of selenocysteine, was easily removed by acidolysis with trimethylsilyl bromide containing *m*-cresol and thioanisole in trifluoroacetic acid. Thus, *p*-methoxybenzyl group can serve as a new protecting group for selenol in peptide synthesis, and can be used for synthesis of various selenocysteine-containing peptides.

Table 7 shows the analytical data for the protected peptides synthesized. Several new techniques recently developed to reduce side reaction during the deprotection were also used in the present synthesis. For example, 1 M trimethylsilyl bromide containing *m*-cresol and thioanisole in trifluoroacetic acid was used as a deprotecting reagent (60). This procedure is more efficient than the previous method with trifluoromethane sulfonate-trifluoroacetic acid (61). In order to avoid possible alkylation of the selenol of selenocysteine residue during the trifluoroacetic acid treatment, anisole (14% by volume) was added to trap *p*-methoxybenzyloxycarbonyl cation produced from the removal of *N*α-*p*-methoxybenzyloxycarbonyl group.

Each diselenide form of glutaselenone were eluted as a single symmetrical peak upon analytical HPLC at the same retention time: 17.0 min (Fig. 11). The oxidized form of glutathione was eluted at the retention time of 14.8 min under the same conditions employed. The final preparation of

Table 7. Analytical data for selenium-containing peptides synthesized.

Compound	M. P. (°C)	$[\alpha]_D^{25}$ (c, in ethyl acetate)	Formula M. W.	Calculated / Found %C	%H	%N
Z(OCH3)-L-SeCys(MBzl)-Gly(OBzl)	72-74	-19.3 (c=0.39)	C29H32N2O7Se	58.10	5.38	4.67
			599.54	58.10	5.38	4.81
Z(OCH3)-D-SeCys(MBzl)-Gly(OBzl)	126-127	22.2 (c=0.51)	C29H32N2O7Se	58.10	5.38	4.67
			599.54	58.46	5.54	5.02
Protected L, L-glutaselenone	132-133	-21.4 (c=0.42)	C37H45O9N3Se	58.88	6.01	5.57
			754.74	58.89	6.12	5.82
Protected D, L-glutaselenone	72-74	-9.6 (c=0.42)	C37H45O9N3Se	58.88	6.01	5.57
			754.74	58.40	5.90	5.82
Protected L, D-glutaselenone	71-72	9.0 (c=0.44)	C37H45O9N3Se	58.88	6.01	5.57
			754.74	58.83	6.07	5.74
Protected D, D-glutaselenone	122-123	20.5 (c=0.56)	C37H45O9N3Se	58.88	6.01	5.57
			754.74	58.81	6.13	5.96

Protected glutaselenone : γ-glutamyl-selenocysteinylglycine

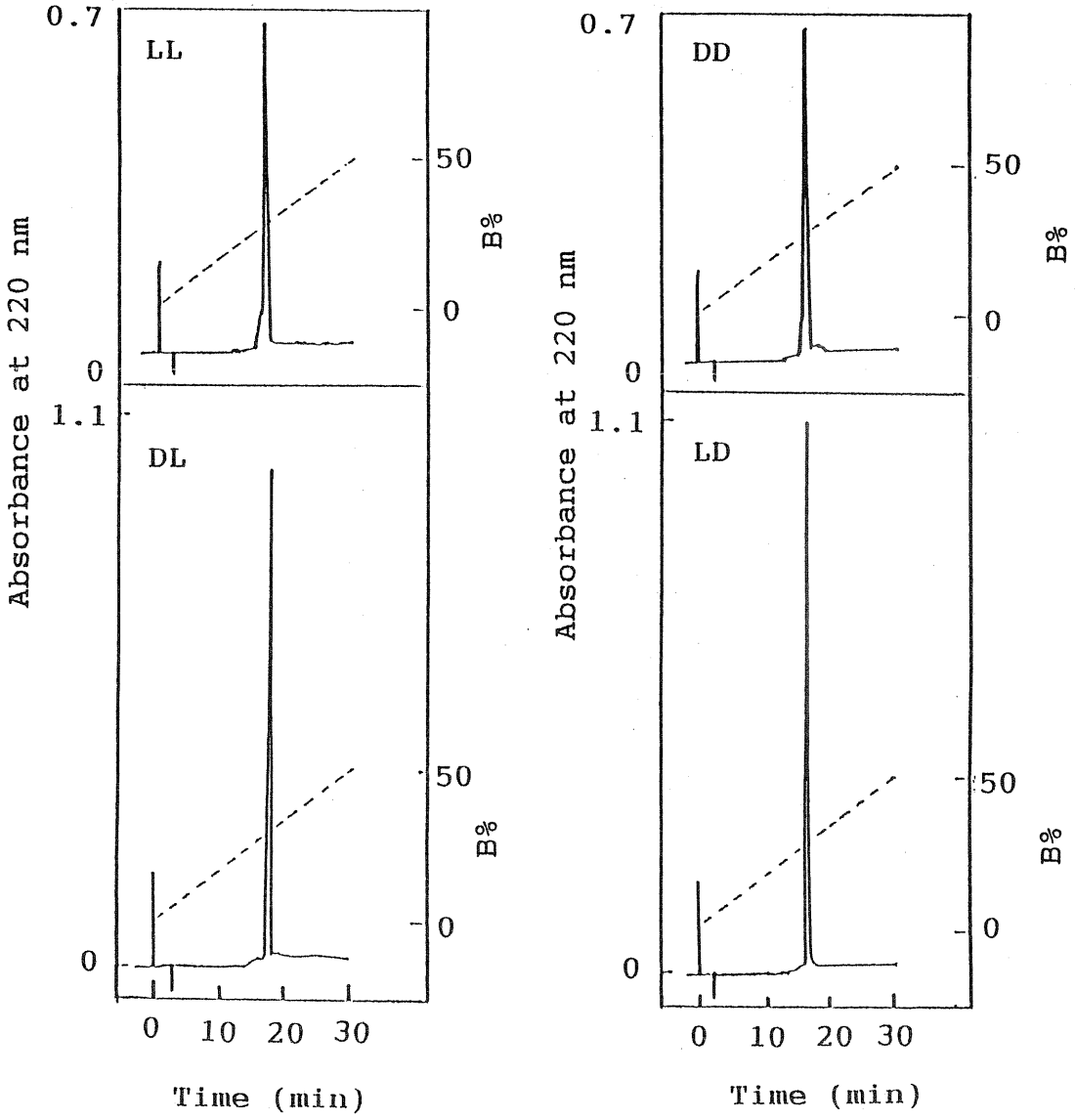

Fig. 11. Reversed phase HPLC profiles of oxidized form of glutaselenone. The column used was COSMOSIL 5C18-AR (Nacalai Tesque, Kyoto, Japan). The elution was programmed at a flow rate of 1.0 ml/min by a linear gradient between 0 and 50% acetonitrile in 0.1% trifluoroacetic acid in water.

glutaselenone was found to be homogeneous by amino acid analysis of the acid hydrolysates (Table 8). Selenocystine was eluted at the retention time of 19.8 min between valine and methionine. The authentic selenocystine was eluted at the same retention time (19.8 min). The average overall yield of the deprotection reaction was about 20% based on the protected glutaselenone.

Table 8. Amino acid analysis of glutaselenone.

	Number of residues				
Amino acid	LL	DL	LD	DD	Calculated
Glu	1.2	1.2	1.2	1.2	1
Gly	1.0	1.0	1.0	1.0	1
SeCys*	0.9	1.1	1.0	1.0	1

*Determined as half selenocystine.

The diselenide form of glutaselenone showed a broad absorption band between 270 and 400 nm with a shoulder around 300 nm (Fig. 12). An extinction coefficient of glutaselenone at 300 nm was calculated to be 870 $M^{-1}cm^{-1}$. The spectrum is similar to that of selenocystine previously reported (62), and the broad absorption band is probably attributable to $n-\sigma^*$ transition of the diselenide bond (63). The diselenide form of glutaselenone showed an emission maximum at 400 and 500 nm when it was excited at 400 nm (Fig. 13). The fluorescence band is also attributable to the transition of diselenide bond.

Each diselenide form of glutaselenone diastereoisomers showed several cotton bands between 210 and 400 nm: LL isomer, 210(-), 230(-), 270(+), and 340(-); LD, 210(+) and 340(+); DL, 210(-) and 340(-); DD, 210(+), 230(+), 270(-), and 340(+), which can be derived from asymmetric carbon atoms of glutaselenone (Fig. 14).

The selenium analogues of several sulfur-containing peptides and proteins have been synthesized. The serine residue at the active center of subtilisin was replaced by selenocysteine residue by chemical modification (23). An analogue of β-galactosidase whose methionine residues were extensively replaced by selenomethionine residue was obtained from a selenium-resistant mutant of *E. coli* grown on a medium containing sodium selenate (64). Selenocysteine analogues of oxytocin (40) and somatostatin (41) were synthesized by liquid phase method. We have synthesized four diastereoisomers of glutaselenone with

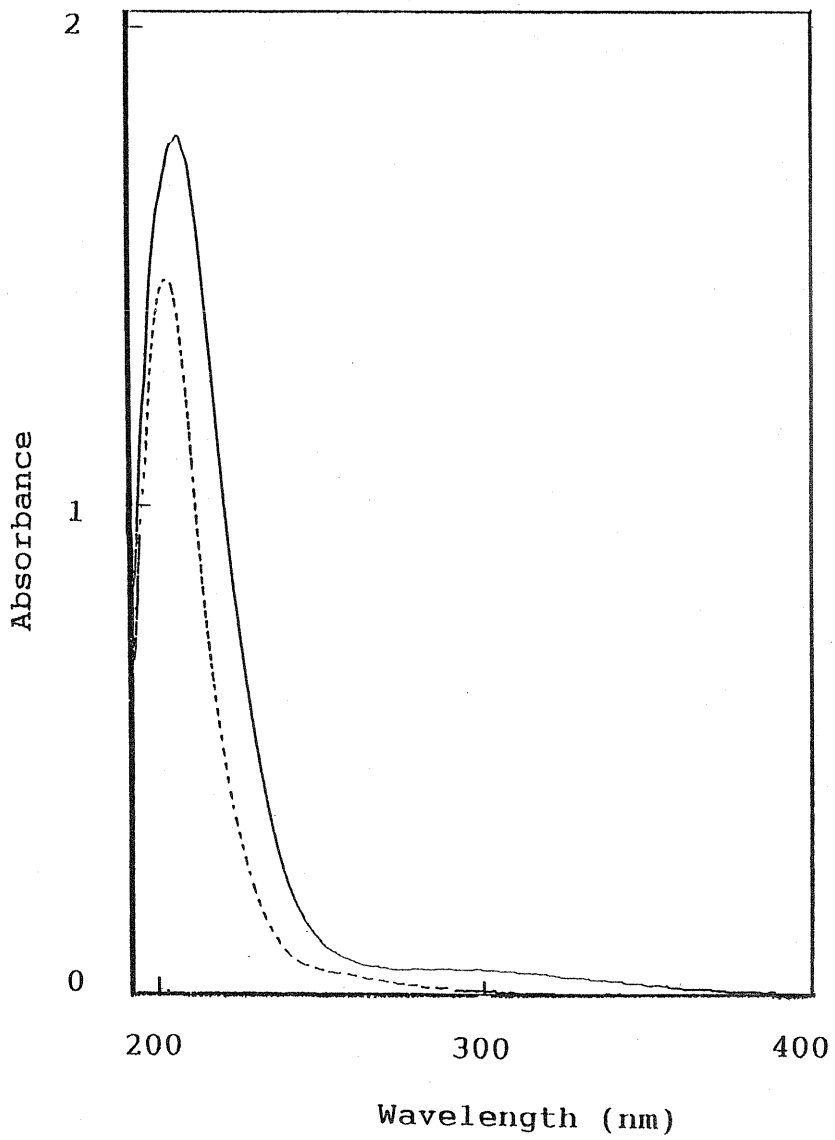

Fig. 12. Absorption spectrum of oxidized form of glutaselenone (———) and glutathione (– – – –): solvent, water; concentration, 1 mg/ml.

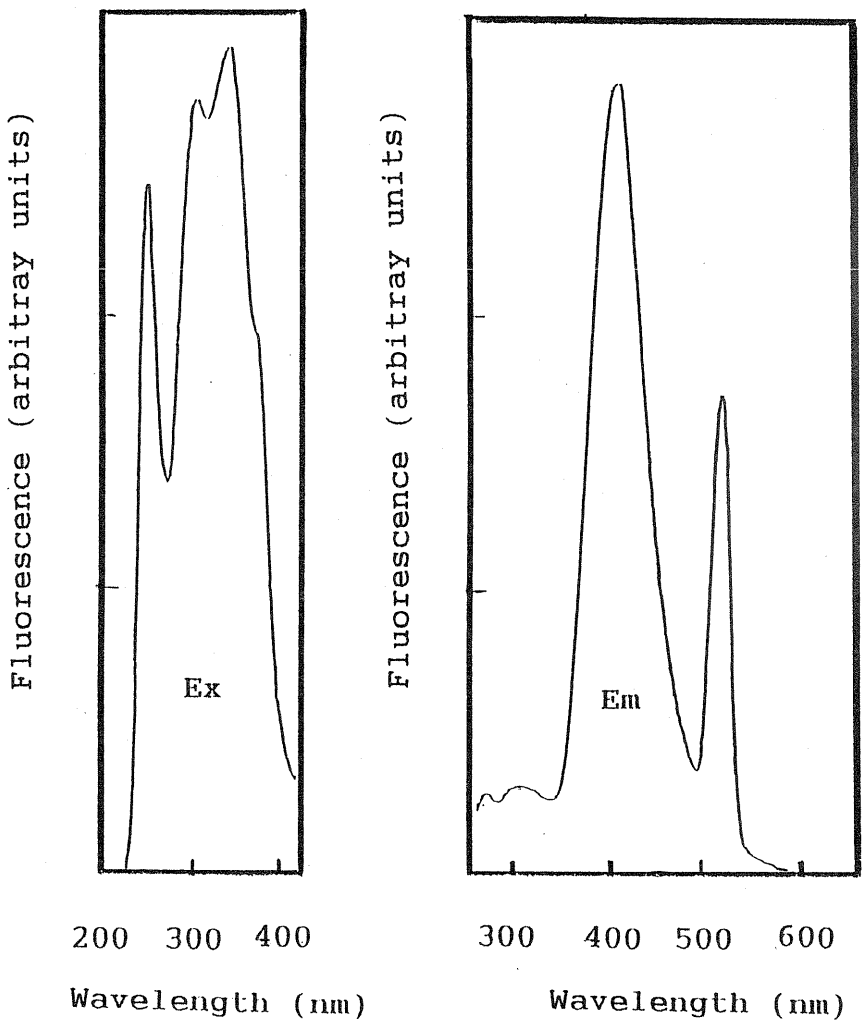

Fig. 13. Emission and excitation spectra of oxidized form of glutaselenone (0.1 mg/ml in water at 25°C). The excitation was done at 400 nm, and the emission was at 245 nm. Em and Ex indicate emission and excitation spectra, respectively.

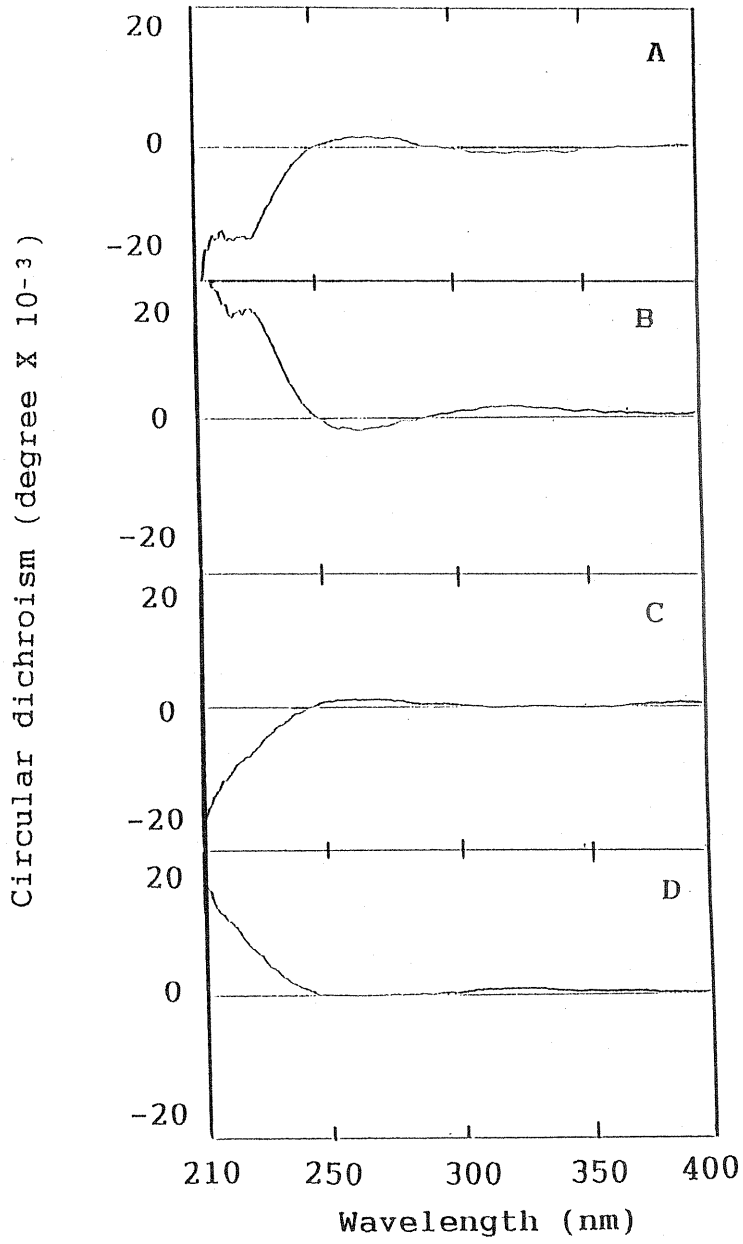

Fig. 14. Circular dichroism of oxidized form of glutaselenone in water. A, 1 mg/ml; L,L-glutaselenone: B, 1 mg/ml; D,D-glutaselenone: C, 0.5 mg/ml; D,L-glutaselenone: D, 0.5 mg/ml; L,D-glutaselenone.

Z(OCH_3)-Secys(MBzl)-OH. This is the first report of synthesis of D-selenocysteine-containing peptides.

Various physiologically-active peptides contain a disulfide bond as an essential moiety (65-67). The formation of disulfide bonds usually proceeds only slowly, and peptides containing disulfide bonds are synthesized with complicated techniques (68, 69). As compared with thiol, selenols are oxidized to form the diselenide much more efficiently (19). Thus, I propose to use selenocysteine instead of cysteine as an analogue of physiologically-active peptides containing essential disulfide bonds. The selenocysteine analogues are expected to show a physiological function similar to the original peptide.

SUMMARY

I synthesized each four diastereoisomers of a selenium analogue of glutathione, LL, LD, DL, and DD-glutaselenone (i.e. γ-L-glutamyl-L-selenocysteinylglycine) separately, using *N*-*p*-methoxybenzyloxycarbonyl-*Se*-*p*-methoxybenzyl-selenocysteine by liquid phase method. The diselenide form of glutaselenone showed a broad absorption band between 270 and 400 nm with a maximum at 300 nm, and a fluorescence emission band at 400 and 500 nm, which can be attributed to diselenide bond. Each diselenide form of glutaselenone showed several cotton bands between 210 and 400 nm: LL isomer, 210(-), 230(-), 270(+), and 340(-); LD, 210(+) and 340(+); DL, 210(-) and 340(-); DD, 210(+), 230(+), 270(-), and 340(+) derived from asymmetric carbon atoms of glutaselenone.

Section 2. Glutathione peroxidase activity of glutaselenone

The reduction of various hydroperoxides by the selenoenzyme glutathione peroxidase has been considered to be a major protective system of mammalian cells against oxidative damages (70). The enzyme is characterized by the active site containing a selenocysteine residue which is essential for the catalytic activity (71).

Recently, Ebselen (2-phenyl-1,2-benzisoselenazol-3(2H)-one) was found to reduce hydroperoxides catalytically (51) in the presence of glutathione by a mechanism similar to that of the mammalian enzyme glutathione peroxidase, and inhibit lipid peroxidation in rat liver microsomes via:

$$2GSH + ROOH \longrightarrow GSSG + ROH + H_2O$$

I here describe glutaselenone catalyzed-glutathione peroxidase activity, and its reaction mechanism.

EXPERIMENTAL PROCEDURES

Materials

Reduced form of glutathione (GSH), oxidized form of glutathione (GSSG), hydrogen peroxide, cumene hydroperoxide, and NADPH were purchased from Nacalai Tesque (Kyoto, Japan): glutathione reductase was from Boehringer Mannheim Yamanouchi (Tokyo, Japan): *t*-butyl hydroperoxide was from Sigma (Missouri, U.S.A.): diphenyl diselenide was from Aldrich (Wisconsin, U.S.A.).

Assays

Glutathione peroxidase activity

Glutathione peroxidase activity was determined by the procedure of Little et al. (72). Oxidized glutathione formed was determined with glutathione reductase, and the rate of NADPH oxidation was measured spectrophotometrically at 340 nm. The assay mixture (1.0 ml) contained 50 mM phosphate buffer (pH 7.0), 1.0 mM GSH, 0.16 mM NADPH, 1.0 mM EDTA, glutathione reductase (0.24 U), and glutaselenone. The reaction was carried out at 37°C, and initiated by the addition of hydroperoxides. The molar absorption coefficient of NADPH used was 6,220 $M^{-1}cm^{-1}$.

Glutathione reductase activity

Glutathione reductase activity was determined by the procedure of Carlberg et al. (73) The assay mixture (1 ml)

contained 50 mM phosphate buffer (pH 7.0), 25 μM GSSG (or GSeSeG), 0.1 mM NADPH, and 1.0 mM EDTA. The reaction was started by addition of glutathione reductase (0.12 U), and carried out at 37°C . The rate of NADPH oxidation was measured spectrophotometrically at 340 nm.

Analytical methods

Enzyme activity was measured with a Shimadzu MPS-2000 spectrophotometer equipped with a water-circulating cell holder.

The reaction mixture was analyzed by reversed phase high performance liquid chromatography (HPLC). Analytical separations were done with a Cosmosil 5C18-AR column (Nacalai Tesque, Kyoto, Japan; 15 X 0.46 cm) at a flow rate of 1.0 ml/min. The column was eluted with 4% acetonitrile in water. Trifluoroacetic acid was added at a concentration of 0.1% (v/v) to water. Peptides were detected at 220 nm.

RESULTS AND DISCUSSION

Glutathione peroxidase activity of glutaselenone

Various organo-selenium compounds showing glutathione peroxidase activity have been previously reported. Diphenyl diselenide showed 1.97 times higher activity than Ebselen (74). The selenium analogues of several sulfur-containing amino acids such as selenocystine and selenocystamine also reduced hydroperoxides

catalytically (75). I have found that each four diastereoisomers of glutaselenone showed glutathione peroxidase activity. This is the first report of selenium-containing peptide showing glutathione peroxidase activity.

I have detected glutathione peroxidase activity of glutaselenone at a concentration of 10^{-5} M Se, and the activity was reduced in the order of LL-, DL-, LD-, and DD-diastereoisomer (Fig. 15). LL-Diastereoisomer showed glutathione peroxidase activity higher than diphenyl diselenide. Selenocystine also showed glutathione peroxidase activity, but no difference in the activity was found between diastereoisomers.

Table 9 shows the molecular activity of various diselenides. The order of glutathione peroxidase activity among four diastereoisomers of glutaselenone did not change with hydroperoxides used. However, the activities for cumene hydroperoxide and *t*-butyl hydroperoxide were lower than that of hydrogen peroxide. In case of LL-glutaselenone, the activities for cumene hydroperoxide and *t*-butyl hydroperoxide were 0.48 and 0.22-fold lower than that of hydrogen peroxide.

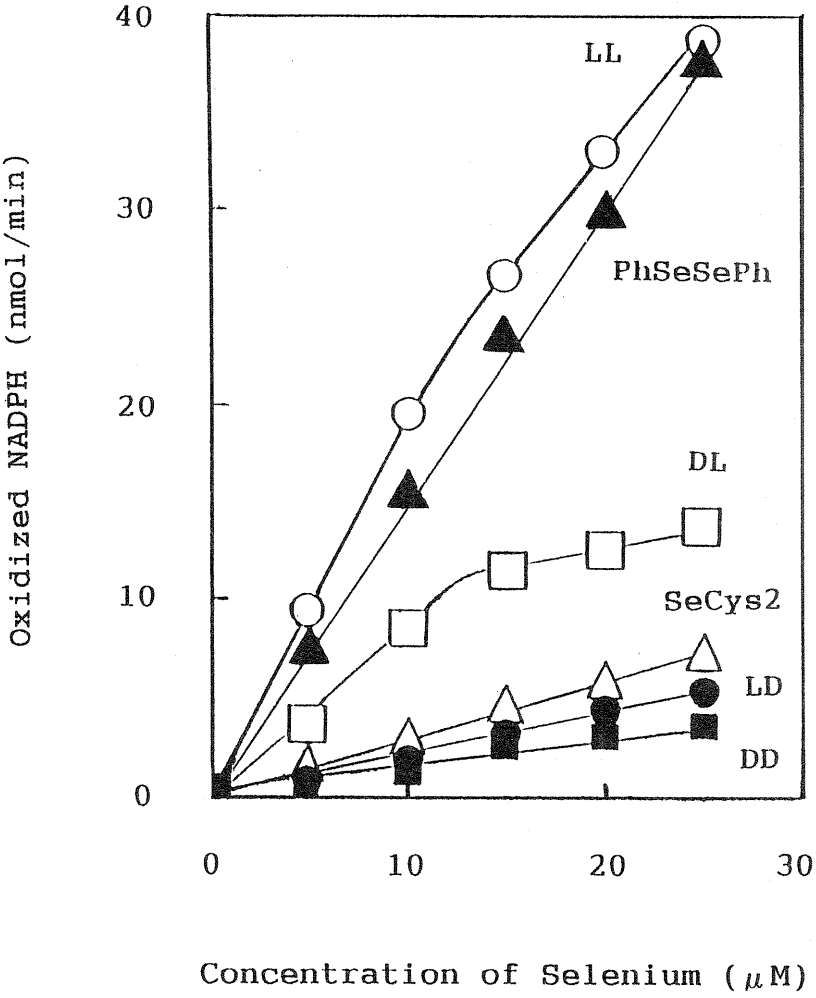

Fig. 15. Glutathione peroxidase activity of glutaselenone Experimental conditions are as follows: GSH, 1 mM; NADPH, 0.16 mM; H_2O_2, 0.2 mM; pH, 7.0; temp., 37°C.

Table 9. The molecular activity of various diselenides.

Se-compound	Molecular activity (min^{-1})		
	H_2O_2	Cumene hydroperoxide	*t*-Butyl hydroperoxide
LL-Glutaselenone	0.97	0.47	0.21
DL-Glutaselenone	0.42	0.23	0.11
LD-Glutaselenone	0.11	0.08	0.04
DD-Glutaselenone	0.07	0.05	0.02
Diphenyl diselenide	0.76	0.54	0.18
Selenocystine	0.14	0.15	0.08

Kinetic constants of glutaselenone-catalyzed glutathione peroxidase activity

Table 10 shows apparent Km values for each four diastereoisomers of glutaselenone for glutathione and hydrogen peroxide. The apparent Km values were increased in the order of LL-, DL-, LD, and DD-diastereoisomer: the affinity for the substrates were decreased in the same order. In the case of LL-glutaselenone, the ratio of the relative Km values for cumene hydroperoxide and *t*-butyl hydroperoxide to hydrogen peroxide were 3.2 and 14.6, respectively. The values are consistent with the hydrophobicity of these hydroperoxides: glutaselenone consists of the hydrophilic amino acids, and probably has a low affinity for the hydrophobic hydroperoxides. The differences in apparent Km values between four diastereoisomers of glutaselenone are most likely due to the difference in the molecular activities between them: the steric hindrance probably makes the total difference in glutathione peroxidase activity between four diastereoisomers of glutaselenone.

Mechanism of the glutaselenone-catalyzed glutathione peroxidase activity

I have shown that each four diastereoisomers of glutaselenone catalyzes the hydroperoxide reduction in the presence of glutathione. Figure 16 shows the proposed mechanism of the glutaselenone-catalyzed glutathione peroxidase activity. Glutaselenone-glutathione selenosulfide (GSeSG) was a stable reaction intermediate, which was eluted between GSSG and GSeSeG by the reversed phase HPLC under the conditions employed. The oxidized form of glutaselenone and GSeSG did not serve as a substrate for glutathione reductase. Another characteristic intermediate, which appeared in the presence of hydrogen peroxide and disappeared by the addition of GSH, was identified as glutaselenone-selenenic acid (GSeOH) by the reversed phase HPLC. Therefore, I propose a mechanism of the glutaselenone-catalyzed glutathione peroxidase activity as follows: the oxidized form of glutaselenone added to the reaction mixture is reduced with glutathione (GSH), and reacts with hydroperoxide to form glutaselenone-selenenic acid (GSeOH); GSeOH reacts with GSH to form glutaselenone-glutathione selenosulfide (GSeSG), and the reduced form of glutaselenone is regenerated through the thiol-selenosulfide interchange reaction between GSeSG and GSH (Fig. 16)

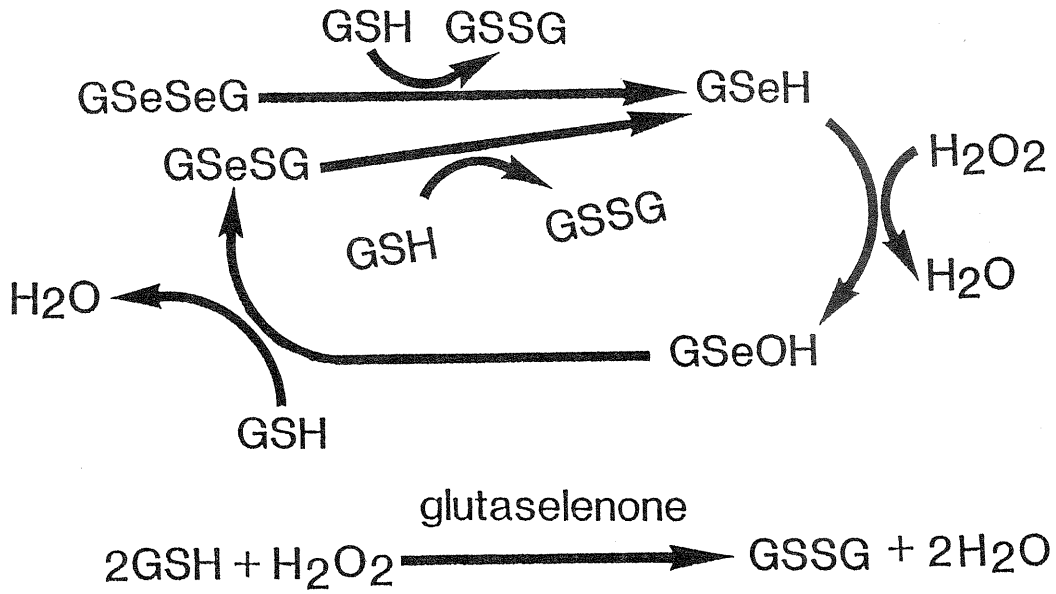

Fig. 16. The proposed mechanism of the glutaselenone-catalyzed glutathione peroxidase activity

SUMMARY

Each four diastereoisomers of glutaselenone was found to reduce various hydroperoxides catalytically in the presence of glutathione by a mechanism similar to that of the mammalian enzyme glutathione peroxidase. The molecular activity of LL-, DL-, LD-, and DD-glutaselenone was determined to be 0.97, 0.42, 0.11, and 0.07 (min^{-1}), respectively, and the apparent Km values were also determined: for GSH (mM), LL-isomer (0.088), DL-isomer (0.23), LD-isomer (0.23), DD-isomer (0.54); for H_2O_2 (mM), LL-isomer (0.10), DL-isomer (0.11), LD-isomer (0.12), DD-isomer (0.28). The steric hindrance probably accounts for the difference in glutathione peroxidase activity between four diastereoisomers of glutaselenone.

ACKNOWLEDGEMENTS

I wish to thank Dr. Kenji Soda, Professor of the Laboratory of Microbial Biochemistry, Institute for Chemical Research, Kyoto University, for his kind guidance and encouragement throughout the course of this work.

I am also grateful to Dr. Nobuyoshi Esaki, Associate Professor of the Laboratory of Microbial Biochemistry, Institute for Chemical Research, Kyoto University, without whose kind advice and encouragement, this work would have not been completed.

The author expresses his deep gratitude to Dr. Hidehiko Tanaka, Professor of the Faculty of Agriculture, Okayama University.

My sincere thanks are due to Dr. Katsuyuki Tanizawa, Associate Professor of Institute of Scientific and Industrial Research, Osaka University.

It is great pleasure to acknowledge the kind advice and encouragement of Dr. Kei Yamanaka, Professor of the Faculty of Engineering, Okayama University of Science.

The author is much indebted to Dr. Hiromu Sakurai (Kyoto Pharmaceutical University), Dr. Tohru Yoshimura (Kyoto University), Dr. Shinji Nagata (Kochi University), Dr. Kenji Inagaki (Okayama University), Dr. Tohru Nakayama (Suntory Ltd.), Dr. Yoshihiro Sawa (Shimane University), Dr. Nobuyoshi Nakajima (Okayama Prefectural Junior College), Dr. Setsuo Furuyoshi (Kyoto

Institute of Technology), Dr. Akira Ohtaka (Kyoto University), Dr. Manabu Sugimoto (Okayama University), Dr. Kumio Yokoigawa (Nara Women's University), Mr. Takashi Tamura (Kyoto University), and Mr. Hiroyuki Ashida (Shimane University).

The author would also thank Mrs. Toshiko Hirasawa and all other members of the Laboratory of Microbial Biochemistry, Institute for Chemical Research, Kyoto University, both past and present, for sharing ideas with me and for the countless other things they have done for me.

Finally, but not the last, I express my deep gratitude to Dr. Minoru Ameyama, Professor of the Faculty of Engineering, Kansai University, for his encouragement.

REFERENCES

1. Shamberger, R. J. (1983) *Biochemistry of Selenium*, Plenum, New York.
2. Committee on Medical and Biologic Effects of Environmental Pollutants, Selenium (1976) *Nat. Acad. Sci.*, Washington, D. C.
3. Nelson, A. A., Fitzhugh, O. G. and Calvery, H. O. (1943) *Cancer Res. 3*, 230.
4. Schwarz, K., and Foltz, C. M. (1957) *J. Am. Chem. Soc. 79*, 3292,
5. Hartley, W. J. and Grant, A. B. (1961) *Fed. Proc. 20*, 679.
6. Patterson, E. L., Milstrey, R., and Stokstad, E. L. R (1957) *Proc. Soc. Exp. Biol. Med. 95*, 617.
7. Rotruck, J. T., Hoekstra, W. G., Pope, A. L., Ganther, H., Swanson, A., and Hafeman, D. (1972) *Fed. Proc. Amer. Soc. Exp. Biol. 31*, 691.
8. Flohe, L., Eisele, B., and Wendel, A. (1971) *Hoppe-Seyler's Z. Physiol. Chem. 352*, 151.
9. Cone, J. E., Martin del Rio, R., Davis, J. N., and Stadtman, T. C. (1976) *Proc. Natl. Acad. Sci. U.S.A. 3*, 2659.
10. Jones, J. B. and Stadtman, T. C. (1981) *J. Biol. Chem. 256*, 656.
11. Ljungdahl, L. G. and Andreesen, J. R. (1978) *Methods Enzymol. 53*, 360.

12. Enoch, H. G. and Lester, R. L. (1975) *J. Biol. Chem. 250*, 6693.

13. Wagner, R. and Andreesen, J. R. (1979) *Arch. Microbiol. 121*, 255.

14. Bradshow, W. H. and Barker, H. A. (1960) *J. Biol. Chem. 235*, 3620.

15. Dilworth, G. L. (1982) *Arch. Biochem. Biophys. 219*, 30.

16. Yamazaki, S. (1982) *J. Biol. Chem. 257*, 7926.

17. Zinoni, F., Birkman, A., Stadtman, T. C., and Bock, A. (1986) *Proc. Natl. Acad. Sci. U.S.A. 83*, 4650.

18. Chambers, I., Frampton, J., Goldfard, P., Affara, N., McBain, W., and Harrison, P. R. (1986) *EMBO J. 5*, 1221.

19. Williams, R. J. P. (1978) *New Trends in Bioinorganic Chemistry*, pp. 253, Academic Press, New York.

20. Berry, M. J., Banu, L., and Larsen, P. R. (1991) *Nature 349*, 438.

21. Read, R., Bellow, T., Yang, J-G., Hill, K.E., Palmer, I. S., and Burk, R. F. (1990) *J. Biol. Chem. 265*, 17899.

22. Stadtman, T. C. (1980) *Ann. Rev. Biochem. 49*, 93.

23. Wu, Z., P. and Hilvert, D.(1989) *J. Am. Chem. Soc. 111*, 4513.

24. Nordberg, M. and Kojima, Y. (1979) in *Metallothionein* (Kagi, J. H. R. and Nordberg, M., Eds.) pp 41, Bairkhauser Verlag, Basel.

25. Walsh, C., Schonbrumm, A., and Abels, R. P. (1971) *J. Biol. Chem. 246*, 6855.

26. Klayman, D. J. and Griffin, S. T. (1973) *J. Am. Chem. Soc. 195*, 197.

27. Chocat, P., Esaki, N., Tanaka, H., and Soda, K. (1985) *Anal. Biochem. 148*, 485.

28. Erickson, B. W. and Merrifield, R. B. (1973) *J. Am. Chem. Soc. 95*, 3757.

29. Nagasawa, T., Kuroiwa, K., Narita, K., and Isowa, Y. (1973) *Bull. Chem. Soc. Japan 46*, 1269.

30. Mitchell, A. R., Kent, S. B. H., Engelhard, M., and Merrifield, R. B. (1978) *J. Org. Chem. 43*, 2845.

31. Sarin, V. K., Kent, S. B. H., Tam, J. P., and Merrifield, R. B. (1981) *Anal. Biochem. 117*, 147.

32. Merrifield, R. B. (1963) *J. Am. Chem. Soc. 85*, 2149.

33. Merrifield, R. B. (1986) *Science* (Washington, D.C.) *232*, 341.

34. Mitchell, A. R., Erickson, B. W., Ryabtsev, M. N., Hodges, R. S., and Merrifield, R. B. (1976) *J. Am. Chem. Soc. 98*, 7357.

35. Tam, J. P., Wong, T. W., Reimen, M. W., Tjoeng, F. S., and Merrifield, R. B. (1979) *Tetrahedron Lett. 20*, 4033.

36. Fee, J. A. and Palmer, G. (1971) *Biochim. Biophys. Acta 245*, 175.

37. Wilson, G. S., Tsibris, J. C. M., and Gunsalus, I. C. (1973) *J. Biol. Chem. 248*, 6059.

38. Meyer, J. and Moulis, M. M. (1981) *Biochem. Biophys. Res. Commun. 103*, 667.

39. Theodoropoulos, D., Schwartz, I. L., and Waltoder, R. (1967) *Biochemistry 6*, 3927.

40. Walter, R. and Chan, W. Y. (1967) *J. Am. Chem. Soc. 89*, 3829.

41. Hartrodt, B., Neubert, K., Bierwolf, B., Blech, W., and Jakubke, H.-P. (1980) *Tetrahedron Lett. 21*, 2393.

42. Popenoe, E. A. and du Vigneaud, V. (1953) *J. Am. Chem. Soc. 75*, 4879.

43. Lerch, K. (1980) *Nature 284*, 368.

44. Kull, F. J., Reed M. F., Elgren, T. E., Ciardelli, T. L., and Wilcox, D. E. (1990) *J. Am. Chem. Soc. 112*, 2291.

45. Smith, T. A., Lerch, K., and Hodgson, K. O. (1986) *Inorg. Chem. 25*, 4677.

46. Goldschmidt, V. M. (1954) *Geochemistry*, Oxford, and references theirin.

47. Sterm, E. A. (1974) *Phys. Rev. B. 10*, 3027.

48. Freedman, J. H., Powers, L., and Peisach, J. (1986) *Biochemistry 25*, 2342.

49. Abrahams, I. L., Bremner, I., Diakun, G. P., Garner, C. D., Hasnain, S. S., Ross, I, and Vasak, M. (1986) *Biochem. J. 236*, 585.

50. Muller, A., Cadenas, E., Graf, P., and Sies, H. (1984) *Biochem. Pharmacol. 33*, 3235.

51. Wendel, A., Fausel, M., Safayhi, H., Tiegs, G., and Otter, R. (1984) *Biochem. Pharmacol. 33*, 3241.

52. Chambers, I., Frampton, J., Goldfarb, P., Affara, N., McBain, W., and Harrison, P. (1986) *EMBO J. 5*, 1221.

53. Meister, A. and Anderson, M. E. (1983) *Ann. Rev. Biochem. 52*, 711.

54. Novi, A. M. (1981) *Science, 212,* 541.

55. Anderson, G. W., Zimmerman, J. E., and Callahan, F. M. (1964) *J. Am. Chem. Soc. 86,* 1839.

56. Simpson, R. J., Neuberger, M. R., and Liu, T.-Y. (1976) *J. Biol Chem. 251,* 1936.

57. Akabori, S., Sakakibara, S., Shimonishi, Y., and Nobuhara, Y. (1964) *Bull. Chem. Soc. Japan 37,* 433.

58. Wilcheck, M., Sarid, S., and Patchornik, A. (1965) *Biochim. Biophys. Acta 104,* 616.

59. Hofmann, K. and Yajima, H. (1961) *J. Am. Chem. Soc. 83,* 2289.

60. Ohtaka, A. (1989) Doctor thesis, Kyoto University, Japan.

61. Yajima, H., Fujii, N., Ogawa, H., and Kawatani, H. (1974) *J. Chem. Soc. Chem. Comm.* 107.

62. Caldwell, K. A. and Tappel, A. L. (1964) *Biochemistry 3,* 1643.

63. Bergson, G., Cleason, G., and Schotte, L. (1962) *Acta Chem. Scand. 16,* 1159.

64. Coch, E, H. and Greene, R., C. (1971) *Biochim. Biophy. Acta, 230,* 223.

65. Moroder, L., Gemeiner, M., Gohring, W., Jager, E., Thamm, P., and Wunsch, E. (1981) *Biopolymers 20,* 17.

66. Siber, P., Kamber, B., Hartmann, A., Johl, A., Riniker, B., and Rittle, W. (1977) *Helv. Chim. Acta 60,* 27.

67. Inukai, N., Nakano, K., and Murakami, M. (1967) *Bull. Chem. Soc. Jpn. 40,* 2913.

68. du Vigneaud, V., Audreith, L. F., and Lorring, H. S. (1930) *J. Am. Chem. Soc. 52*, 4500.

69. Kamber, B. and Riltel, W. (1968) *Helv. Chim. Acta 51*, 2061.

70. Parnham, M. J. and Graf, E. (1987) *Biochem. Pharmacol. 36*, 3095.

71. Epp. O., Ladenstein, R., and Wendel, A. (1983) *Eur. J. Biochem. 133*, 51.

72. Little, C. and O'Brien, P. J. (1968) *Biochem. Biophys. Res. Commun. 31*, 145.

73. Carlberg, I. and Mannerrik, B. (1985) *Methods Enzymol. 113*, 484.

74. Wilson, S. R., Zucker, P. A., Huang, R. -R. C., and Spector, A. (1989) *J. Am. Chem. Soc. 111*, 5936.

75. Yasuda, K., Watanabe, H., Yamazaki, S., and Toda, S. (1980) *Biochem. Biophy. Res. Commun. 96*, 243.